

# ASTEROSEISMOLOGY OF CEPHEIDS

ENNIO PORETTI

*Osservatorio Astronomico di Brera*

*Via E. Bianchi, 46 - 23807 Merate, Italy*

## 1. Introduction

The importance of Cepheids is well known in many fields of astronomy. In this contribution I would like to show how it is possible to obtain indications about the internal structure of a Cepheid and how we can test models of this class of variable stars.

Section 2 introduces the Fourier decomposition, a tool to describe quantitatively the light curves of pulsating stars. In the past years I have been involved in a project concerning Cepheids with  $P < 8$  d and in Sect. 3 I will show how an observational result was progressively built on the basis of old and new data; the latter were collected on selected targets just to clarify some controversial points. Since different pulsation modes were suspected among these stars, an independent confirmation was searched for.

To do that we applied the least-squares technique to Double Mode Cepheids. By obtaining a very satisfactory description of their pulsational content (Sect. 4), we demonstrated how powerful the method is. Moreover, we could confirm that between Cepheids with  $P < 8$  d they are both fundamental and first overtone pulsators (Sect. 5). The detection of small amplitude cross-coupling terms and higher harmonics in the light curves of Double Mode Cepheids allowed us to quantify the properties of the high-order terms and hence to discover other peculiarities (Sect. 6), very useful to complete the scenario of the resonance effects and to test some theoretical models (Sect. 7).

## 2. The application of Fourier decomposition to Cepheid light curves

Following the notation proposed by Simon and Lee (1981), the Fourier decomposition consists in interpolating the measurements by means of the

series

$$V(t) = A_o + \sum_{i=1}^N A_i \cos[2\pi i(t - T_o)f + \phi_i] \quad (1)$$

$V(t)$  is the magnitude observed at times  $t$ ,  $A_o$  the mean magnitude,  $A_i$  the amplitudes of each component,  $f$  the frequency ( $f=1/P$ , where  $P$  is the period of the light variation),  $\phi_i$  the  $i$ -th phase at  $t = T_o$ . The components  $2f, 3f, 4f \dots$  are the first, second, third ... harmonics of the main frequency  $f$ . Note that the use of the `sin` term instead of the `cos` one can lead to spurious results, owing to the  $\pi/2$  shift of the phase component. Another trouble can originate from a different formula, for example considering  $2\pi\phi_i$  in the development.

This technique provides quantitative parameters to define the shape of the light curves and it is therefore a powerful tool for classification purposes. The Fourier parameters can be subdivided into two groups: the amplitude ratios  $R_{ij} = A_i/A_j$  (i.e.  $R_{21} = A_2/A_1$ ,  $R_{31} = A_3/A_1$ ,  $R_{32} = A_3/A_2$ , ...) and the phase shifts  $\phi_{ji} = i\phi_j - j\phi_i$  (i.e.  $\phi_{21}=\phi_2 - 2\phi_1$ ,  $\phi_{31}=\phi_3 - 3\phi_1$ ,  $\phi_{32} = 2\phi_3 - 3\phi_2$ , ...).

Figure 1 shows how the light curve of a pulsating stars is progressively changed by adding harmonic terms. The upper panel represents a perfect sine-shaped curve having frequency  $f$ . When adding the first harmonic  $2f$  ( $R_{21}=0.30$  and  $\phi_{21}=4.5$  rad), the light curve immediately becomes asymmetrical (middle panel). Adding the second harmonic  $2f$  ( $R_{31}=0.10$  and  $\phi_{31}=2.5$  rad), the brightness increase is again much steeper; the effect of higher harmonics is to originate curves which are even again more asymmetrical (i.e. with a decreasing  $M - m$  value, where  $M$  is the phase of maximum brightness and  $m$  the phase of minimum brightness) and to fit some small jumps of the light curves. The case of S Cru ( $P=4.68997$  d, 6<sup>th</sup> order fit) is shown in Fig. 2.

### 3. The application to Cepheids with $P < 8$ d

We could verify that the sequence formed by the classical Cepheids is very narrow and it can be described by the linear fit

$$\phi_{21} = 3.332 + 0.216 P \quad (2)$$

This fit is the mathematical representation of the well-known Hertzsprung progression. An observed scatter of 0.30 rad in the  $\phi_{21}$  value puts a star well outside of the progression. By applying the Fourier decomposition to all the available light curves of Cepheids with  $P < 8$  d, we could evidence two other sequences: an upper one with  $2.0 \text{ d} < P < 3.5 \text{ d}$ ,  $\phi_{21} > 4.2$  rad and a lower one with  $3.0 \text{ d} < P < 5.5 \text{ d}$ ,  $\phi_{21} < 4.0$  rad (Fig. 3, first panel). The

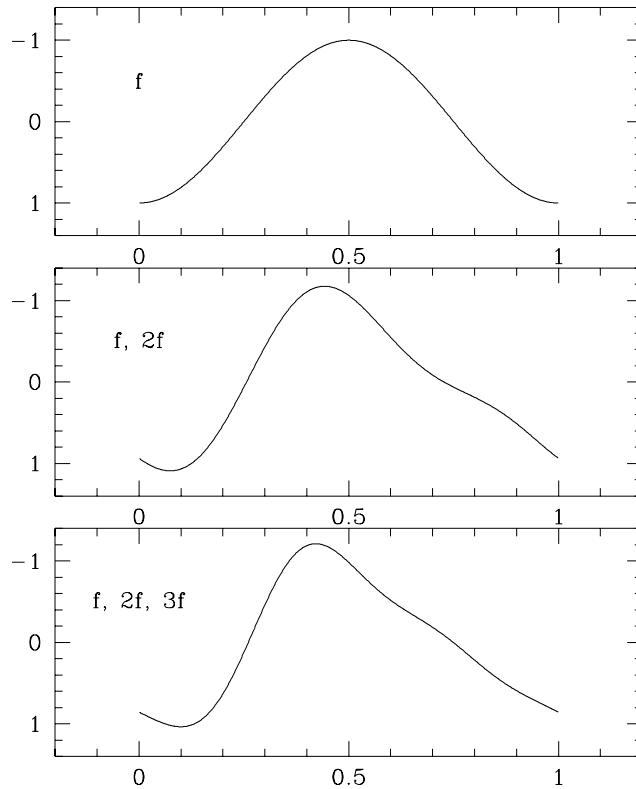


Figure 1. Changes in the light curve by adding to a sine-shaped term (upper panel) its first harmonic  $2f$  (medium panel) and its second harmonic  $3f$  (lower panel)

four panels of Fig. 3 show the successive modifications of the  $\phi_{21}-P$  plot from the first analysis (Antonello & Poretti 1986) to the last one (Poretti 1994).

After the first work, it was not evident what was the reason for the three sequences. Gieren et al. (1990) showed that the stars located on the upper sequence are pulsating in the first overtone mode. Different interpretations were proposed for the stars located on the lower sequence: Gieren et al. (1990) suggested that these stars are fundamental pulsators but differ from classical Cepheids for another reason, perhaps a different  $M-L$  relationship. Antonello et al. (1990) suggested the presence of a resonance between the first and a higher overtone at  $P \approx 3$  d. They also called  $C-a$  stars those forming the classical progression and  $C-b$  stars those forming the upper and lower sequences. Let us consider hereinafter this latter nomenclature; in Sect. 6 we shall define the pulsational properties of the Cepheids and we

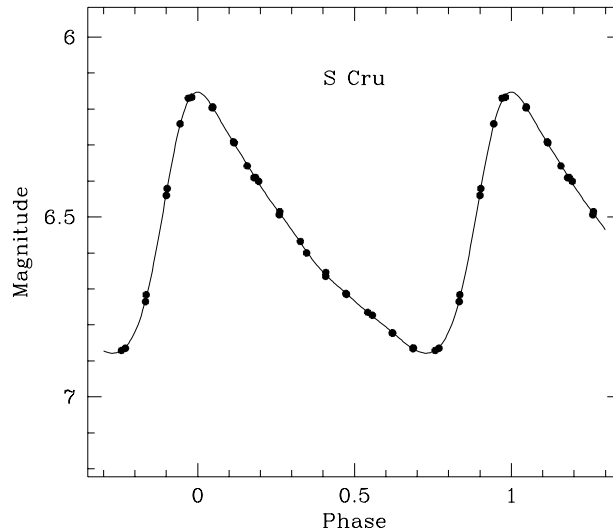


Figure 2. The light curve of S Cru: a 6<sup>th</sup>-order fit is necessary to fit the steep rising branch

shall propose a unique classification.

The controversial aspects of the matter were an incentive to observing a greater number of Cepheids. The upper and lower sequences were not as defined as the other one; hence we decided to perform new decompositions and, if necessary, new observations. For this reason our group supplied very accurate photoelectric photometry of some selected stars whose position was not very clear in the Fourier parameter spaces.

The new observational data collected by Mantegazza & Poretti (1992) brought some clarification into the matter. The link between the two sequences could be established by considering the  $\phi_{31}-P$  plane. In this plane the progression is continuous and it is formed by stars located on the upper and lower sequences in the  $\phi_{21}-P$  plane. Hence, all the  $C - b$  stars have a common nature. But the  $\phi_{21}$  sequence is really interrupted by a resonance? To verify this point, let us consider the case of BY Cas. Its  $\phi_{21}$  value is quite normal (Fig.4, left panel), as it is located on the  $C - a$  sequence; however, its  $\phi_{31}$  value falls exactly on the  $C - b$  sequence (Fig. 4, right panel). It is quite evident that a star falling on the resonance interval can display any  $\phi_{21}$  value: a very high one, as the stars on the upper sequence do, a very low one, as the stars in the lower sequence do, a “ $C - a$ ” one, as BY Cas does. This is the signature of a resonance.

Hence, we can summarize 6 years of investigations on the light curves

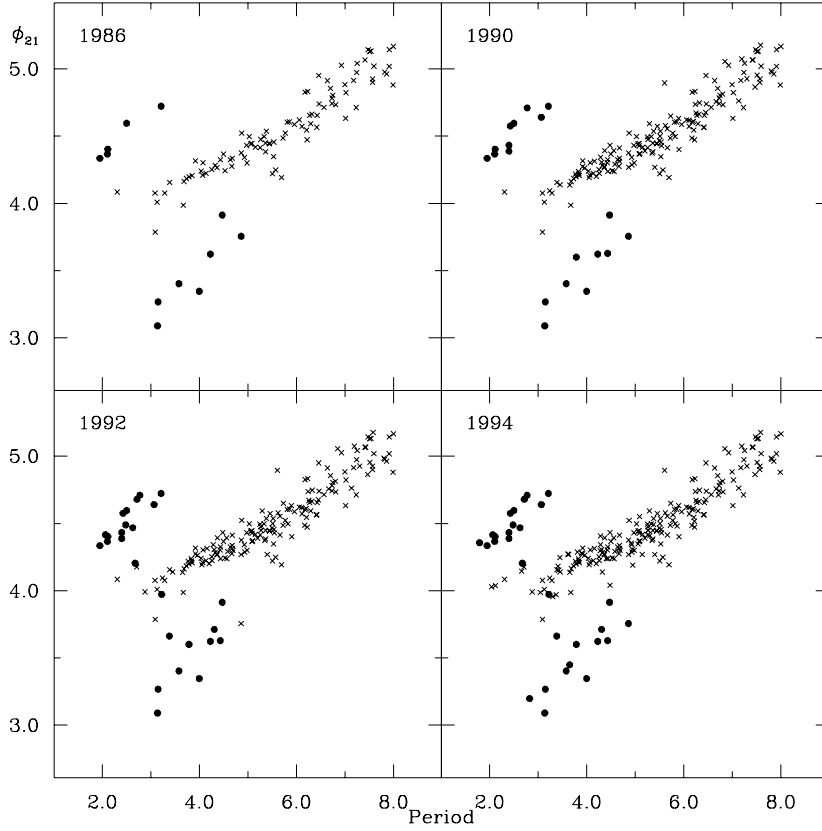
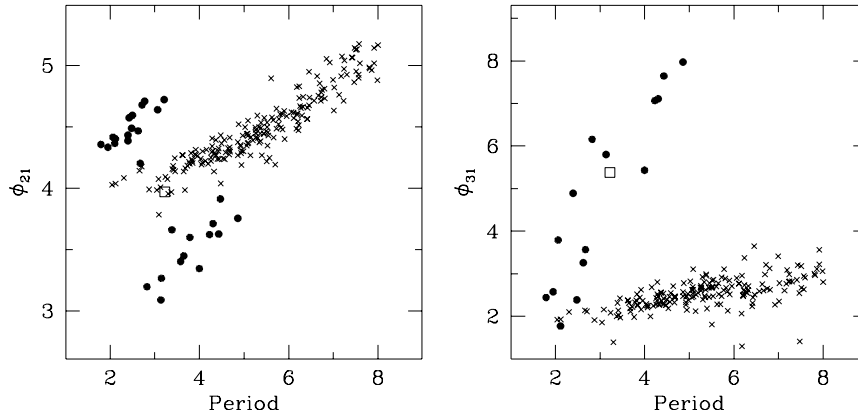


Figure 3. The  $\phi_{21}-P$  plot and its modifications from 1986 to 1994. It is an example of growing confidence in a feature, i.e. the “Z”-shaped progression crossing the classical, linear one.

of Cepheids with  $P < 8$  d in this way:

- The  $\phi_{31}-P$  plane strengthens the hypothesis that  $C-b$  stars (i.e. the stars forming the upper and lower sequences in the  $\phi_{21}-P$  plane) have a common nature;
- The case of BY Cas demonstrates that at  $P \approx 3$  d the  $\phi_{21}$  values are spread over a wide interval. The two sequences are then ideally connected; this is the fingerprint of a resonance;
- Since the theoretical models of Cepheids do not support resonances at  $P \approx 3$  d involving the fundamental mode, we are forced to consider  $C-b$  stars as first overtone pulsators;
- the  $C-a$  stars are fundamental mode pulsators, the  $C-b$  stars are



*Figure 4.* The  $\phi_{31}$ - $P$  plot shows the connection between the stars on the upper and lower sequences of the  $\phi_{21}$ - $P$  plot. The enlarged squares indicate the phase values of BY Cas

first-overtone pulsators. The  $\phi_{21}$  values can then be successfully used to discriminate between pulsation modes.

Hence, the suggestion firstly made by Antonello et al. (1990) was confirmed. The effect of the  $P \approx 3$  d resonance was the same as the one observed for the classical Cepheid sequence at  $P \approx 10$  d; the complication here is the simultaneous presence of the two classes of pulsators, which partly masks the discontinuity.

Looking at Fig. 5 we can compare the light curves of two Cepheids having similar periods, but belonging the one to the  $F$ -pulsator class (BE Mon,  $P=2.705510$  d) and one to the  $1O$ -pulsator class (V526 Mon,  $P=2.674985$  d). As can be easily noted, the light curve of BE Mon is much more asymmetric and moreover the maximum is sharper.

#### 4. The double-mode Cepheids: the detection of the frequency content

The Double-Mode Cepheids (DMCs) supply the laboratory where the conclusions described in the previous sections can be verified: it is a well established fact that in 13 cases out of 14 the two excited modes are the fundamental and the first overtone mode. The light curve of a DMC can be considered as the sum of the contributions of a set of frequencies. Two are really independent ( $f_1$  and  $f_2$ ); since each of the corresponding curves is not perfectly sine-shaped, the harmonics  $2f_1, 3f_1, \dots, 2f_2, 3f_2, \dots$  are also observed. Moreover, the two independent modes are interacting and

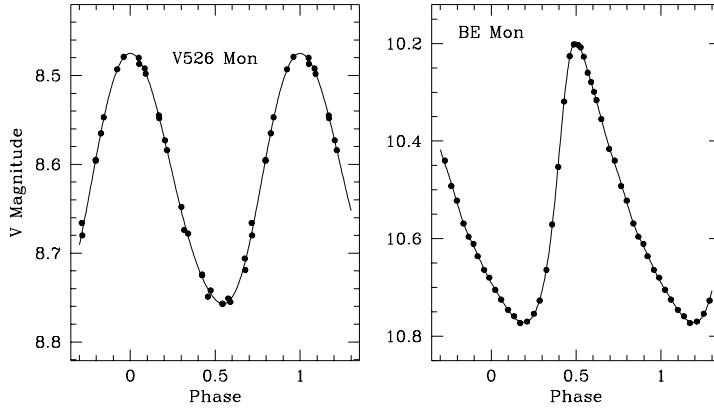


*Figure 5.* The light curves of a Cepheid pulsating in the first overtone (V526 Mon, left panel) is quite different from that of a Cepheid pulsating in the fundamental one (BE Mon, right panel). The two stars have the same period, around 2.7 d. Data were collected at ESO: the standard deviation of the fit is 4.5 mmag for V526 Mon and 2.9 mmag for BE Mon

the cross coupling terms are observed; they are defined as  $|if_1 \pm jf_2|$  (i.e.  $f_2 - f_1$ ,  $f_1 + f_2$ ,  $2f_1 + f_2$ ,  $2f_2 - f_1$  and so on). Pardo & Poretti (1997) submitted all the available photometry on DMCs to a frequency analysis with the following objectives:

- to quantitatively determine the importance of harmonics and of the cross-coupling terms;
- to compare the Fourier parameters with those of  $C - a$  and  $C - b$  stars;
- to search for the fingerprints of resonances between modes, by using Fourier parameter plots;
- to establish properties of Fourier parameters as a function of their order.

In the approach to the light curve analysis we took advantage of our experience on small amplitude pulsating variables ( $\delta$  Sct and  $\gamma$  Dor stars). As a matter of fact, after finding the main constituents, the other terms have a very small amplitude and a well tested procedure is recommended to detect them in a reliable way. Hence, we used the least-squares power spectrum method (Vanicek 1971). Let us discuss the methodology in detail using the available measurements on VX Pup. In the first power spectrum of Fig. 6 the peak at  $f_1 = 0.3320 \text{ cd}^{-1}$  and its alias at  $1.33 \text{ cd}^{-1}$  are clearly visible. The aliases are particularly strong in this dataset since the measurements were obtained in a single site; when merging measurements obtained at two or more sites the height of the aliases will decrease. Then

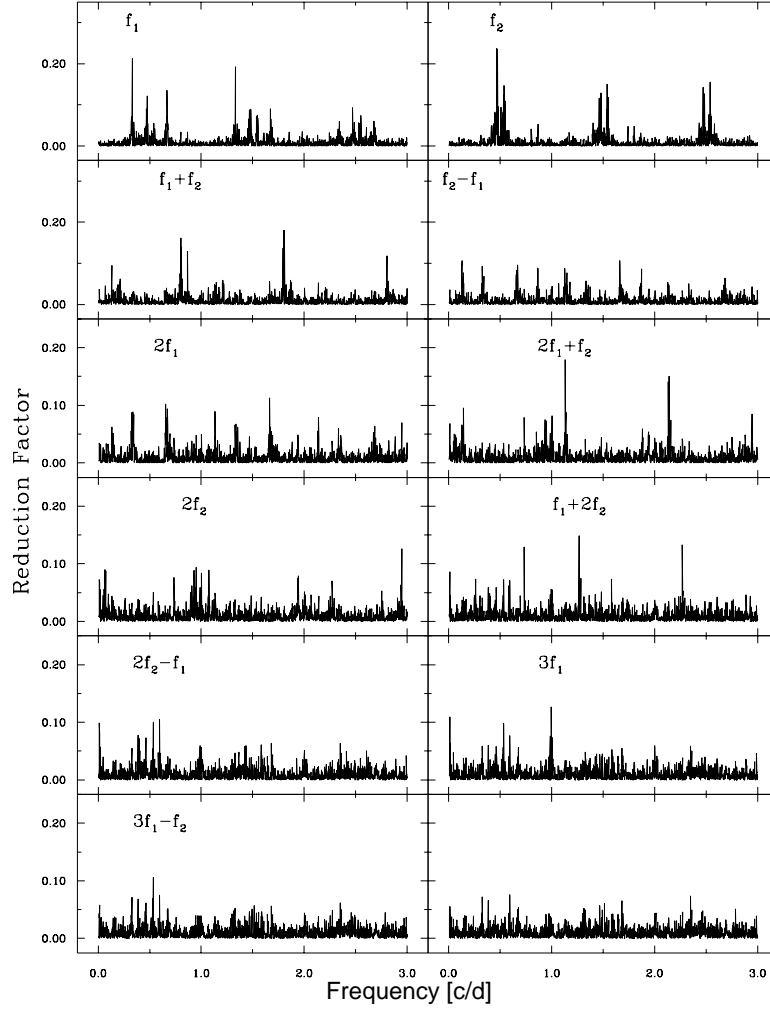


*Figure 6.* Power spectra of the VX Pup measurements. Each panel shows the spectrum obtained by introducing all the terms identified as known constituents in the previous ones; this means that their frequencies are considered as established, but their amplitude and phase values are recalculated for each new frequency

we introduced  $f_1$  as a known constituent (hereinafter k.c.) searching for the second term: in the second power spectrum the  $f_2=0.4674 \text{ cd}^{-1}$  term and its whole alias structure appeared (i.e. the  $1-f$ ,  $f+1$ ,  $2-f$ ,  $f+2$ ,  $3-f$  terms). It is important to note that no prewhitening was done: only the frequency value  $f_1$  was considered as a k.c. and in the second search the unknowns were  $V_o, A_1, \phi_1, f_2, A_2, \phi_2$ . Before proceeding further with a new frequency



search, the values of  $f_1$  and  $f_2$  were refined by a simultaneous least-squares fit and then they were introduced as k.c. in the third search, which allowed us to detect the  $f_1 + f_2$  term (third panel). Now, frequency refinement is a delicate step because the third component must always satisfy the relationship  $f_1 + f_2$ ; to do this refinement, we use the MTRAP code (Carpino et al. 1987) which keeps this relationship locked throughout the best fit search. After the refinement, we introduced the  $f_1$ ,  $f_2$ ,  $f_1 + f_2$  terms as k.c.'s ( $V_o, A_1, \phi_1, A_2, \phi_2, A_{f_1+f_2}, \phi_{f_1+f_2}, f_3, A_3, \phi_3$  are the unknowns) searching for the new light curve component: we detected  $f_2 - f_1$ . Once again, the refinement was performed by keeping the  $f_1 + f_2$  and  $f_2 - f_1$  relationships locked; new frequency values were then obtained and introduced as k.c.'s, the fifth component  $2f_1$  was detected and so on. Following this process, we detected 11 terms. We note that in some spectra, especially in the  $f_1 + f_2$  and  $2f_1$  cases, the highest peaks are not the expected term, but their alias at  $1 \text{ cd}^{-1}$ . This overtaking is due to the interaction between noise and spectral window (we were dealing here with single-site measurements). When observing this event, the exact value of the expected term is considered to proceed further. The decision to stop the term selection was taken when no more term was visible over the noise distribution, i.e. when all the terms giving a significant contribution to the light curve shape were presumably identified. In Fig. 6 the 12<sup>th</sup> panel clearly shows that no other term can be detected in a clear way as the noise distribution is quite uniform. Of course, very small amplitude terms can remain hidden in the noise level, especially when dealing with inaccurate measurements.

## 5. Comparison between double- and single-mode Cepheids

In the previous sections we mentioned the separation between  $C - a$  and  $C - b$  stars in the space of the Fourier parameters. The very reliable Fourier parameters now at our disposal for the galactic DMCs allow us to give an independent confirmation of the proposed interpretations. Figure 7 shows the distribution of the  $\phi_{21}$  values of the galactic DMCs superimposed to the single-mode ones. The  $\phi_{21}$  values corresponding to the  $F$  radial mode occupy the same region as the Classical Cepheids. In like manner, the  $\phi_{21}$  values of the the  $1O$  radial mode mimics the “Z” shape: note the overlap between DMCs and  $C - b$  in the upper part, the high value at 3.0 d (BQ Ser) and the positioning of the two  $\phi_{21}$  values belonging to the longest period DMCs (EW and V367 Sct) just on the lower part. It appears quite evident that in the DMCs the light curves of the  $F$ -radial mode and the  $1O$ -mode are very similar to the curves of the  $C - a$  and  $C - b$ , respectively. In turn, this fact proves without any doubt that  $C - b$  stars are pulsating in the  $1O$  mode and that the  $\phi_{21}$  value can be considered a powerful discriminant

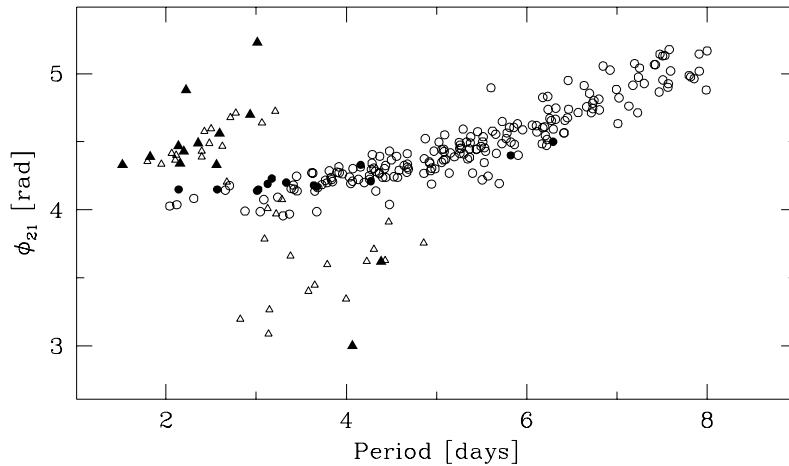


Figure 7. The  $\phi_{21}-P$  plot. Dots: single mode  $C-a$  Cepheids. Triangles: single mode  $C-b$  Cepheids. Filled dots: fundamental radial modes of DMCs. Filled triangles: 1O radial modes of DMCs

between these modes. It should be also noted that the  $F$ -mode light curve of a DMC follows the Hertzsprung progression. A discontinuity is present near 3.0 d in the light curves of 1O modes of DMCs.

As a result of our step-by-step analysis, we can conclude that Cepheids can be subdivided into two groups on the basis of the different pulsation mode:

- the fundamental radial mode pulsators. They are classified as CEP by the GCVS, are the Classical Cepheids in the current literature and are designed as  $C-a$  stars in Antonello et al. (1990);
- the first overtone radial mode pulsators. They are classified as DCEPS by the GCVS, are the  $s$ -Cepheids in the current literature and are designed as  $C-b$  stars in Antonello et al. (1990).

It should be noted that the old definition of  $s$ -Cepheid, i.e. a star showing a sinusoidal light curve, should now be dropped as too generic. The Fourier decomposition supplies us with a quantitative tool to describe it and small asymmetries can be measured. As Fig. 8 shows, the stars forming the “Z” sequence also show a small  $R_{21}$  value and hence the light curve deviates very slightly from a sinewave shape. However, it can be noted as the  $R_{21}$  values for the  $F$ -mode of some DMCs are smaller than the expected ones. We stressed once more that the Fourier parameters have to be considered globally to perform a reliable identification.

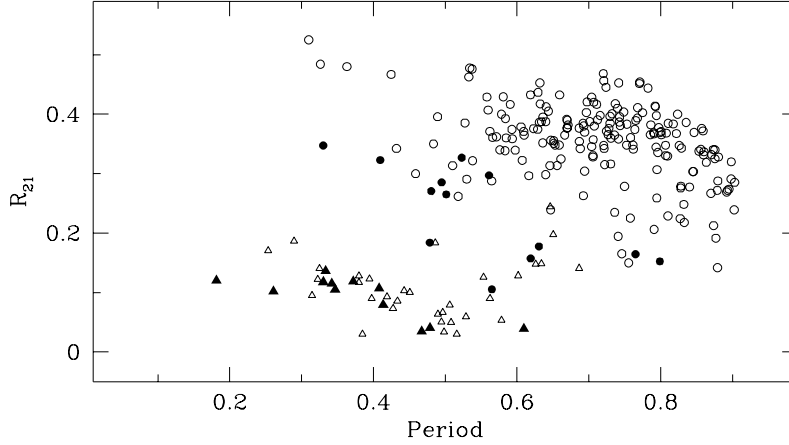


Figure 8. The  $R_{21} - P$  plot. Dots: single mode  $C - a$  Cepheids. Triangles: single mode  $C - b$  Cepheids. Filled dots: fundamental radial modes of DMCs. Filled triangles: 10 radial modes of DMCs

## 6. The generalized phase differences

Pardo & Poretti (1997) fitted the  $V$  magnitudes of DMC by means of the formula

$$V(t) = V_o + \sum_z A_z \cos[2\pi f_z(t - T_o) + \phi_z] \quad (3)$$

where  $f_z$  is the generic frequency, which can be an independent frequency ( $f_1$  and  $f_2$ ), a harmonic or a cross coupling term. Their analysis demonstrated that each component in the DMC light curves can be defined as a combination of two basic frequencies  $f_1$  and  $f_2$ ; by defining  $z = (i, j)$ , we have  $f_z = f_{i,j} = i f_1 + j f_2$ . Some examples: for  $(i, j) = 2, 0$  we have the harmonic  $2f_1$ ; for  $(i, j) = 1, 1$  the  $f_1 + f_2$  term; for  $(i, j) = -1, 1$  the  $f_2 - f_1$  term; for  $(i, j) = 3, -2$  the  $3f_1 - 2f_2$  and so on.

In order to define the properties of the Fourier parameters of the DMC light curves it is very useful to recall to mind the *generalized phase differences* introduced by Antonello (1994b), here noted as  $G_{i,j}$ . They are a linear combination of the phases of each term  $f_{i,j}$  and of the phases  $\Phi_1$  and  $\Phi_2$  of the independent frequencies  $f_1$  and  $f_2$ . Their expression is given by

$$G_{i,j} = \phi_{i,j} - i\Phi_1 - j\Phi_2 + 2k\pi \quad (4)$$

The numerical application to the U TrA fit provides some examples (the integer  $k$  values have to be selected so that  $G_{i,j} \in [0, 2\pi]$ ):

$$G_{1,1} = \phi_{1,1} - \Phi_1 - \Phi_2 + 2k\pi =$$

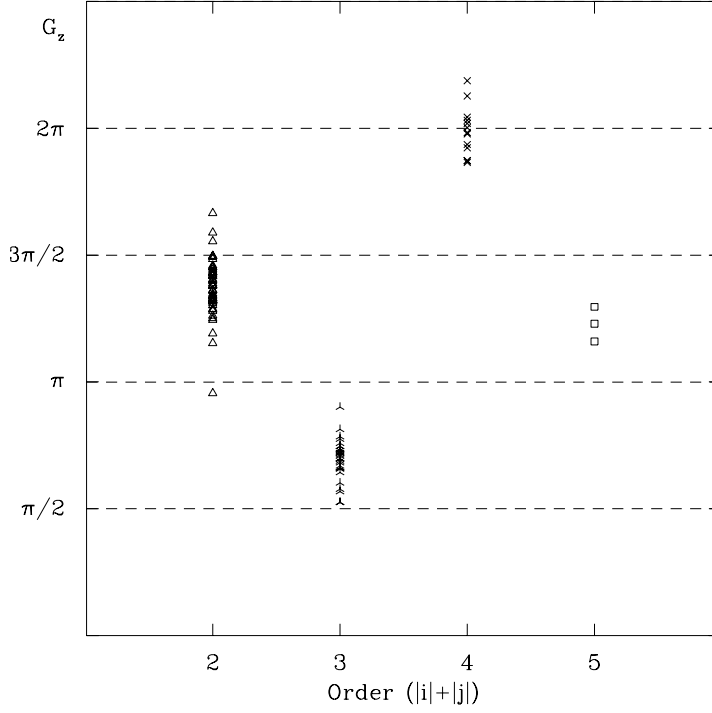


*Figure 9.* The regularity in the Fourier parameters is emphasized when plotting the generalized phase differences  $G_{i,j}$  as function of the order. This also means that light curves are predictable. The spread of the 2<sup>nd</sup> order values is discussed in the text

$$= 2.93 - 5.20 - 6.25 + 4\pi = 4.04$$

$$\begin{aligned} G_{-1,1} &= \phi_{-1,1} + \Phi_1 - \Phi_2 + 2k\pi = \\ &= 4.79 + 5.20 - 6.25 = 3.74 \end{aligned}$$

$$\begin{aligned} G_{4,1} &= \phi_{4,1} - 4\Phi_1 - \Phi_2 + 2k\pi = \\ &= 6.00 - 4 \cdot 5.20 - 6.25 + 8\pi = 4.07 \end{aligned}$$

It is quite interesting to plot the  $G_{i,j}$  values against their fit order. Light curves of DMCs are often quoted as an example of erratic behaviour and cycle-to-cycle variations, both in amplitude and in phase. Pardo & Poretti (1997) have already proved that these light curves seem to be much more stable than reported and that a frequency locked fit yields a satisfactory representation.

The suspicion that the DMC light curves have a predictable behaviour is confirmed by the natural upper and lower limits that can be easily observed in Fig. 9. The second order terms are confined in the region just below  $3/2\pi$ ; the third order terms have  $\pi/2 < G_{i,j} < \pi$ , the fourth order ones cluster around  $2\pi$  (or 0), the fifth order ones seem to have  $\pi < G_{i,j} < 3/2\pi$ .

The mean  $G_{i,j}$  values are  $4.30 \pm 0.34$  rad for the second order (i.e.  $|i| + |j| = 2$ ),  $2.20 \pm 0.23$  rad for the third one,  $6.24 \pm 0.31$  for the fourth one,  $3.85 \pm 0.21$  for the fifth one. These mean values are roughly equispaced, with a slight tendency to increase: indeed, the differences between the mean  $G_{i,j}$  of adjacent orders are 2.10, 2.24, 2.39 rad, respectively. The latter result and the boundary values established above yield an experimental confirmation of the rule of uniformity of phase differences in monoperoiodic Cepheids. However, the observed separation ( $\sim 2.2$  rad) is a bit larger than expected ( $\pi/2$ ) in the case of adiabatic pulsations in a one-zone model (see Poretti & Pardo 1997 for a more detailed discussion).

The second order  $G_{i,j}$  values ( $2f_1, f_1 + f_2, f_2 - f_1, 2f_2$ ) range from 3.00 to 5.23 rad; it was expected to see a little spread of the  $G_{0,2}$  values owing to the resonance at 3.0 d. Indeed the two extrema are just related to the  $2f_2$  components of the BQ Ser (the DMC approaching resonance from the shorter periods) and EW Sct (the DMC approaching resonance from the longer periods) light curves. Antonello (1994a) reported another possible resonance between the third overtone and the  $f_1 + f_2$  term near 6.5 d; Fig. 10 definitely proves it. The last point ( $4.02 \pm 0.09$  rad, V367 Sct,  $P=6.293$  d) is clearly out of the progression followed by the other points. Combined with the progressive weakening of the amplitude of the  $f_1 + f_2$  term, this fact strongly supports the action of a resonance effect involving the  $f_1 + f_2$  term.

## 7. The resonance signatures and the influence on the models

There are many effects ascribed to resonances between modes:

1. The evidence of the resonance at  $P \approx 10$  d was firstly evidenced by Simon & Lee (1981). The values of the  $\phi_{21}$  parameter were spread on a very large interval and the progression is abruptly interrupted. The involved modes are the second overtone and the fundamental mode ( $2O/F=2$ );
2. In this paper we reconstructed the methodological procedure used to show how we recognized the effect of the resonance at  $P \approx 3$  d in the 1O pulsator light curves; the involved modes are the fourth and the first overtone. Aikawa (1993) tried to obtain the first implications of its effect in nonlinear models;
3. A resonance is expected around 6–7 d for fundamental pulsators, involving the fourth overtone and the fundamental modes (Moskalik et al

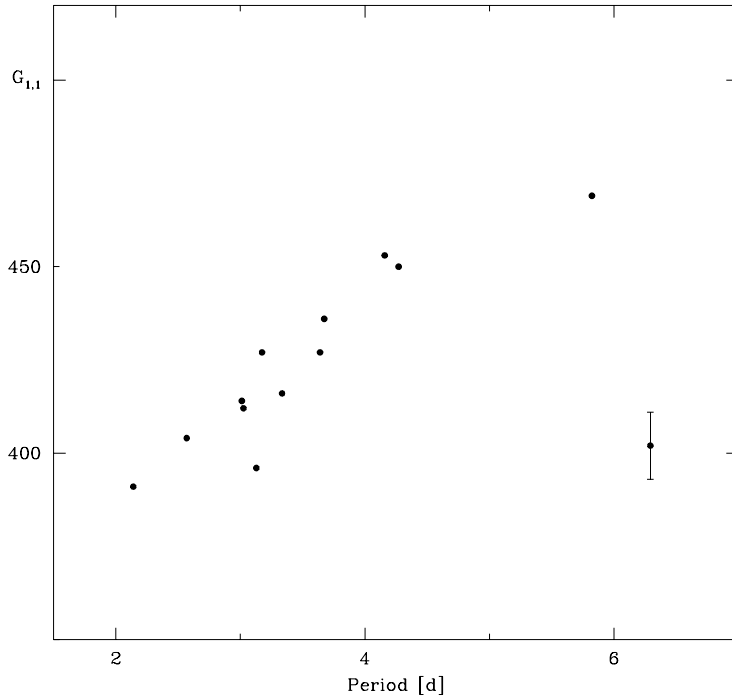


*Figure 10.* The  $G_{1,1}$  progression related to the coupling term  $f_1+f_2$ . Note how the last point (related to V367 Sct) appears to deviate strongly. This can be explained by a resonance acting at  $P \approx 6.0$  d

- 1989). The small feature related to it was noted by Antonello (1994a);
4. As regards the DMCs, the Fourier decomposition of the light curve of V367 Sct suggests a possible resonance around 6.5 d. In such a case, the cross-coupling term  $f_1+f_2$  and the third overtone were involved;
  5. When considering longer periods, features suggesting the action of two resonances were observed (Antonello & Morelli 1997). The fundamental and the third overtone are the involved modes for that at  $P \approx 27$  d ( $3O/F=3$ ), while the fundamental and the first overtone are those for that at  $P \approx 24$  d ( $1O/F= 3/2$ )

It should be noted that their effects are not very strong and a careful analysis is necessary to identify them. Moreover, other dedicated, photometric observations can be useful. For an application of the same technique to radial velocity curves and related results see Kienzle et al. (1999).

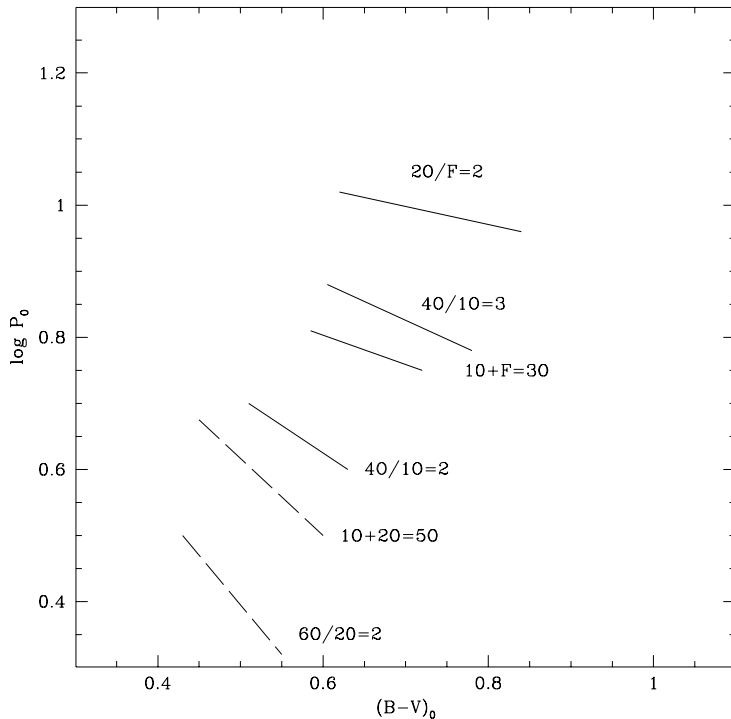


Figure 11. The resonances predicted by the linear model combined with nonstandard  $M - L$  relationship are shown.  $F$  indicates the fundamental radial mode;  $1O$ ,  $2O$ ,  $3O$  the first, second, third... radial overtones. Dashed lines indicated resonances not (yet?) observed

Figure 11 shows the positions of the resonances and the involved modes in a  $(B - V) - P$  plot. They were predicted by linear models and for nonstandard Mass-Luminosity relationship. Theoretical models can be obtained by varying some input parameters as opacity, overshooting effects,  $M - L$  relationship. A general agreement between theoretical models and observational effects was found. Sequences of models were realized using both standard and overshooting-type  $M - L$  relationships (Antonello 1997). Other models were obtained by using different artificial viscosity parameters and temperature values. In all these cases the theoretical light curves were decomposed and the Fourier parameters straightly compared with the observed ones. Recent results indicated that the models with mild overshooting have  $M - L$  relationships in better agreement with observations than others based on standard assumptions (Antonello 1997).

## 8. Conclusion

This paper shows how the analysis of the light curves can be used to probe the structure of the Cepheids. Therefore, we can study the Cepheids from the point of view of

*asteroseismology*

since to find resonance effects is as to sound stellar interiors. The discontinuities at  $P \approx 10$  d and  $P \approx 3$  d were confirmed by the data obtained in the framework of large-scale projects as MACHO and EROS (observations of Cepheids located in the Small and Large Magellanic Clouds). It will be interesting to carefully check also the other in the same large databases.

## References

- Aikawa T., 1993, ApSS 210, 269  
Antonello E., 1994a, A&A 282, 835  
Antonello E., 1994b, A&A 291, 820  
Antonello E., 1997, in *A Half Century of Stellar Pulsation Interpretations: a tribute to Arthur N. Cox*, P.A. Bradley and J.A. Guzik eds., ASP Conf. Ser. vol. 135, p. 243  
Antonello E., Morelli P.L., 1996, A&A 314, 541  
Antonello E., Poretti E., 1986, A&A 169, 149  
Antonello E., Poretti E., Reduzzi L., 1990, A&A 236, 168  
Carpino M., Milani A., Nobili A.M., 1987, A&A 181, 182  
Gieren W.P., Moffett T.J., Barnes T.G., Matthews J.M., Frueh M.L., 1990, AJ 99, 1196  
Kienzle F., Moskalik P., Bersier D., Pont E., 1999, A&A 341, 818  
Mantegazza L., Poretti E., 1992, A&A 261, 137  
Moskalik P., Buchler J.R., 1989, ApJ 341, 997  
Pardo I., Poretti E., 1997, A&A 324, 121  
Poretti E., 1994, A&A 285, 524  
Poretti E., Pardo I., 1997, A&A 324, 133  
Simon N.R., Lee A.S., 1981, ApJ 248, 291  
Vanicek V., 1971, ApSS 12, 10